PAPER • OPEN ACCESS

Soft sensing force measurement approach in sheet metal forming facilities

To cite this article: Jon Olaizola *et al* 2020 *IOP Conf. Ser.: Mater. Sci. Eng.* **967** 012015

Soft sensing force measurement approach in sheet metal forming facilities

Jon Olaizola[a], Aitzol Iturrospe[a], Jose Manuel Abete[a], Lander Galdos[a] and Eneko Sáenz de Argandoña[a]*

[a] *Mondragon Unibertsitatea, Loramendi 4, Mondragon 20500, Gipuzkoa, Spain*
* *esaenzdeargan@mondragon.edu*

Keywords: Stamping force, soft sensors, real time monitoring

Abstract. Process stability and facility security are the two main purposes for measuring the force in sheet metal forming facilities. These two purposes look for guaranteeing the good health of the facility avoiding overloads and at the same time look for variations in the process force that could lead to products out of the demanded quality. Traditionally there have been different approaches to measure the force exerted by the press. Piezoelectric sensors and strain gages are the most widely used technologies. However there are some common limitations that reduce the success in the measurement of the force by the aforementioned sensors: force sensors tend to have a signal drift and the introduction of the sensors together with the electronics represents an extra cost that in some cases can be high. As an alternative to the implementation of force sensors, soft sensing approaches take advantage of the already available signals in the facility to estimate non measured variables, the force in this case. The present work aims at predicting the force curve that a servo press exerts in forming processes reading the internal servomotor signals. The approach has been evaluated with several forming processes achieving an error lower than 3% for all the cases.

1. Introduction

Monitoring plays a crucial role in modern industrial processes and machines. It provides useful information about the condition of the machine and the process quality. Furthermore, monitoring can detect signs of malfunction that may cause the machine's failure and its subsequent downtime. In the specific case of a servo press, a press that is driven by a servo motor, the process force has a high impact in the quality of the manufactured part. The monitoring of the force can reveal aspects related to the quality of the produced part, such as information about the profile of the applied force that it was subjected to during a stroke. The industry's classical approach for monitoring press force is to place sensors on machine components. Due to ease of installation and the little wear they suffer compared with other locations, such sensors are commonly installed on the press frame and the connecting rods [1]. However, force sensors located in forming tools provide more precise information, since they are closer to the process. When the tool is replaced to produce a new component, these sensors are usually replaced, which increases the cost of monitoring [1]. These sensors also experience higher levels of wear than those mounted on the frame or connecting rods. It is also well known that force sensors tend to lose their initial calibration over the working cycles, and they need periodic maintenance for recalibration [2].

IOP Conf. Series: Materials Science and Engineering **967** (2020) 012015 doi:10.1088/1757-899X/967/1/012015

To address the increased costs and the recalibration need associated with physical sensors, other solutions, such as model-based soft(ware) sensors (MBSS), can be adopted, which take advantage of the already existing signals and a model of the targeted machine. A MBSS is a software-based sensor that uses a mathematical representation (model) of the machine and/or process and some measurements to provide estimations [3]. Models are described by state variables (also known as states, as an example the ram position or velocity) that determine the behaviour of the system. At the same time, the system can be driven by external inputs. Those inputs can be either known or unknown depending on whether they are measured or unmeasured. In the case of servo presses, the press force is modelled as an unmeasured input. The signals utilized by the control of the system (in this case torque and angular position of the servomotor) can be used by soft sensors to estimate states and the unknown input (unmeasured force) of the servo press.

In this paper the dual particle filter algorithm presented by [4] has been employed to monitor different metal forming processes. The dual particle filter is an algorithm able to estimate in real time both the states of the system as well as the unknown inputs. Therefore, it takes advantage of the already available signals of the system provided by the installed sensors, avoiding the installation of new ones. The rest of the paper is organized as follows. Section II presents the model of the servo press. Section III briefly describes the proposed dPF-based approach. Section IV shows the experimental results of three different experiments conducted for three different metal forming operations. Finally, Section V provides the conclusions that were extracted from the developed work.

2. Servo press model

A servo press is formed by mechanical and electric components so that it can perform the forming of workpieces. Its operation is powered by a servomotor which creates a rotary motion that is translated into the linear motion of the ram by means of the kinematic chain that is in between. Permanent magnets synchronous motors (PMSP) are the most widely used servomotors to feed servo presses. PMSMs are conventionally controlled by the field oriented control scheme, which takes advantage of the servomotor's angular position and electric signals such as voltages and currents of the different phases that are present in the servomotor.

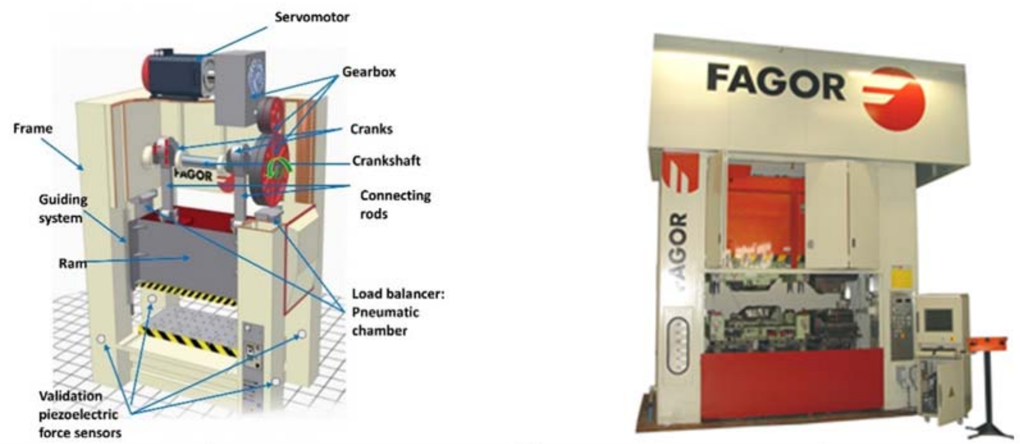

Press capacity (kN)	*4,000 at 20 mm from the BDC*
Number of connection rods	*2*
Working torque Maximum / Nominal (N.m)	*5,5000 / 3,000*
Max stroke (mm)	*400*
Die height (mm)	*1,000 to 1,2000 (str 400mm)*
Stroke adjustment (mm)	*200*

Table size (mm x mm)	*2,400 x 1,200*
Max number of stroke (spm)	*40*
Die cushion capacity (kN)	*400*
Die cushion stroke (mm)	*150*
Main motor power Maximum / Nominal (kW)	*450 / 250*

Figure 1. Components and characteristics of Fagor Arrasate's SDM2-400-2400-1200 servo press.

The mechanical part of the servo press is based on a ram-crank mechanism, as illustrated in Figure 1. Its transmission chain is comprised of a gearbox, a crankshaft, two connecting rods and a ram, which transforms the electric torque τ_e generated by the servomotor into a linear force. A load balancer is also included in the model, since it actuates in the real system compensating the weight of the ram. The model also integrates a friction model that explains some of the friction phenomena affecting the performance of the servo press. The components and characteristics of the servo press used at the present research work are shown in Figure 1. The schematic representation of the mechanical components of the servo press and the complete modelling of the servo press are shown in Figure 2. The modelling of a ram-crank type servo press was carried out by the Lagrange method presented in [5] and [6]. All the components considered in the model are shown in left side of Figure 2 and its representation in the model is shown in right side of Figure 2. All symbols in the modelling equation can be found in [4].

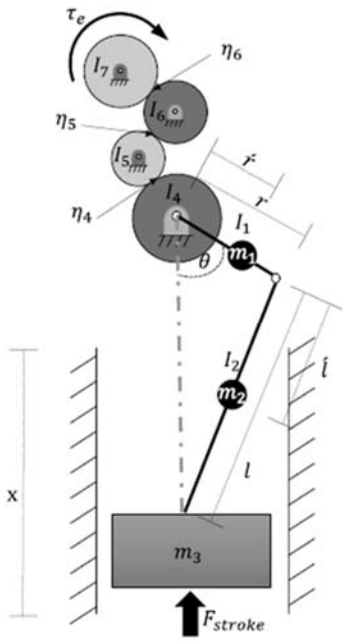

$$
\begin{aligned}
&\ddot{\theta}\Bigg(I_1 + m_1\acute{r}^2 + \frac{I_2 r^2\cos^2\theta}{c^2} + \frac{(l-\acute{l})^2}{l^2} m_2 r^2\cos^2\theta \\
&+ \sin^2\theta\left(m_2 r^2\frac{(r\acute{l}\cos\theta + lc)^2}{l^2c^2} + m_3 r^2\frac{(r\cos\theta + c)^2}{c^2}\right) + I_4 \\
&+ I_5\eta_4^2 + I_6(\eta_4\eta_5)^2 + I_7(\eta_4\eta_5\eta_6)^2\Bigg) \\
&+ \frac{1}{2}\dot{\theta}^2\Bigg(\frac{2I_2 r^4\cos^3\theta\sin\theta}{c^4} - \frac{2I_2 r^2\cos\theta\sin\theta}{c^2} \\
&- \frac{2m_2 r^2\cos\theta\sin\theta\,(l-\acute{l})^2}{l^2} \\
&+ 2\sin\theta\cos\theta\left(m_2 r^2\frac{(r\acute{l}\cos\theta + lc)^2}{l^2c^2} + m_3 r^2\frac{(r\cos\theta + c)^2}{c^2}\right) \\
&+ 2\sin^2\theta\Bigg(\frac{m_2 r^3\acute{l}\sin\theta\,(r\acute{l}\cos\theta + lc)(r\cos\theta - c)(r\cos\theta + c)}{l^2c^4} \\
&+ \frac{m_3 r^3\sin\theta\,(r\cos\theta - c)^2(r\cos\theta + c)^2}{c^4}\Bigg)\Bigg) \\
&+ g\left(\sin\theta\,(m_1\acute{r} + m_2 r + m_3 r) + \sin\theta\cos\theta\left(\frac{m_2 r^2\acute{l}}{lc} + \frac{m_3 r^2}{c}\right)\right) \\
&= \tau_e\eta - \tau_{fric} - (F_{stroke} + F_{lb} + F_{fric})\, r\sin\theta\left(1 + \frac{r\cos\theta}{c}\right)
\end{aligned}
$$

Figure 2. Schematic representation of the mechanical components of the servo press (left side) and the complete model of the servo press (right side).

The servo press model is used to generate the predictions of the magnitudes of interest of the system so that the soft sensor can make inferences from those predictions and obtain the desired estimations of the dynamic response of the servo press and the process force.

3. The soft sensor: the dual particle filter

The employed algorithm, the dual particle filter (dPF) is based on the conventional particle filter (PF) algorithm which was originally formulated for the estimation of the system states that explain the dynamic response of the system, such as the angular position, angular speed and acceleration of the crankshaft of the servo press. The dual scheme of the dPF integrates two PFs, making the algorithm able to estimate not only the states of the system but also an unknown input such as the process force of the servo press.

The workflow of the algorithm is shown in Figure 3. Each PF of the dPF performs four steps to carry out the estimation of states: the Prediction & Update step, the Normalization step, the Resampling step and the Averaging step, as described in [4].

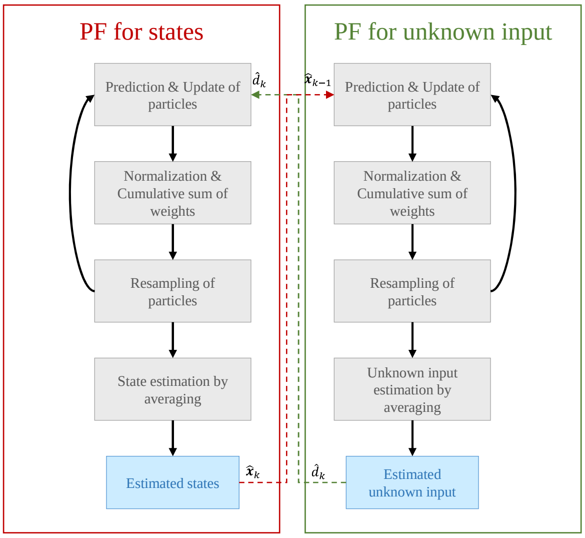

Figure 3. Workflow of the employed dPF.

4. Experimental results

The dPF was evaluated under three different industrial processes. Two measurements were employed to feed the model: the three phase currents and the angular position of the servomotor. The estimated process force was compared with actual force signals measured by two piezoelectric sensors installed in drilled holes of the two connecting rods of the servo press. The evaluated industrial processes are shown next.

4.1 Single strokes against rigid cylinders

In this process, the ram applies the force against two rigid cylinders that are placed on the ram right under the connection rods of the servo press. The main purpose of the experiments was to generate a parabolic force curve that is not very complex in shape but changes very rapidly in time. This way, the response of the prediction algorithm to sudden force changes wanted to be analyzed. The servo press was working at a cadence of 6 strokes per minute in these tests.

The maximum load that the servo press can perform is 400 t. In order to evaluate the algorithm at several force levels, four different set-ups were analysed. In order to modify the press force the ram position with respect the connection rods was changed at each of the set-ups. Several tests were carried out in order to evaluate the repeatability of the prediction algorithm finding similar results between them.

Table 1 gathers the methodological set-up to carry out the four different force levels in the experiments.

Experiment	Maximum force measured	Adjustment of ram (height)	Angular speed during force profile
STR1	88.65 t	848.0 mm	36 °/s
STR2	184.27 t	847.6 mm	36 °/s
STR3	232.19 t	847.3 mm	36 °/s
STR4	343.11 t	846.6 mm	36 °/s

Figure 4 shows four measured and estimated process forces of four different experiments with their corresponding instantaneous normalised absolute deviations. The instantaneous absolute normalised deviation is obtained by means of the absolute value of the difference between the estimated and measured signals, normalised with a factor of 400 t, which is the maximum load capacity of the servo press. The maximum deviation shown in the highest force point is given in the fourth experiment, 2.97%. Apart from that some fluctuation emerge around the 0º angular position of the crankshaft. This is due to control's activity to correct the speed deviation that occurs as the structure recovers from its elastic deformation. The control system of the servomotor was not included in the model due to the lack of information.

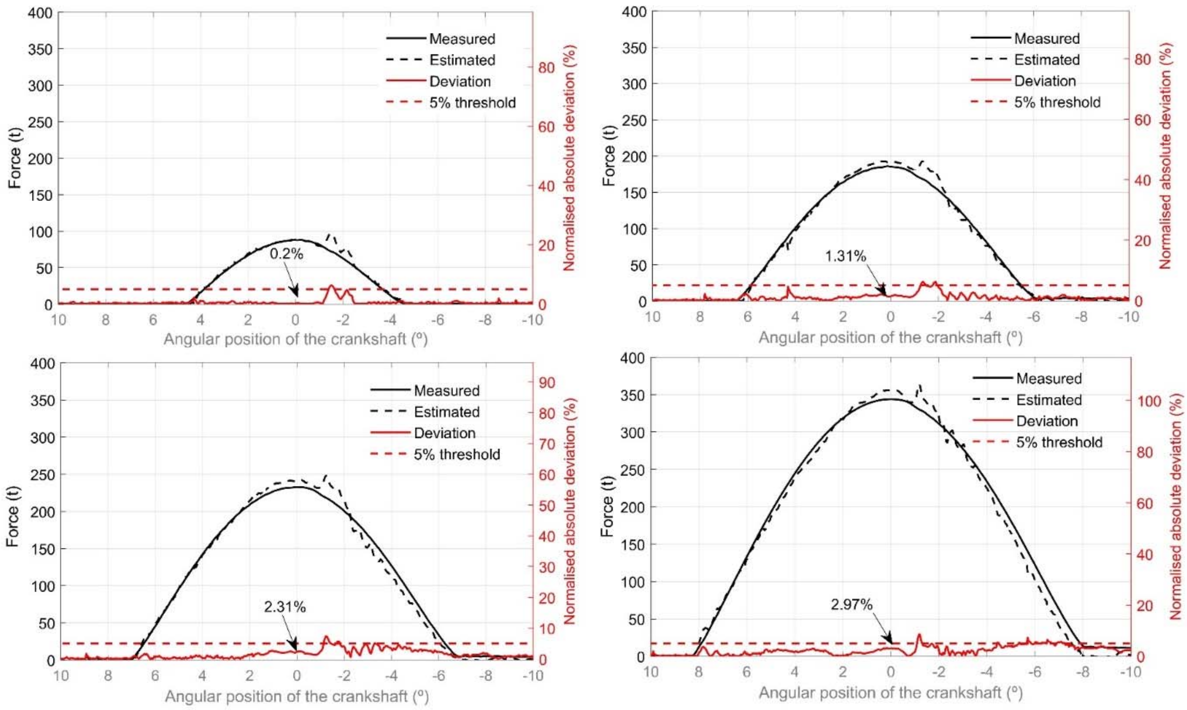

Figure 4. Measured and estimated process forces of the four experiments and the instantaneous normalised absolute deviation.

4.2 Deep drawing processes

The second type of process that was carried out to evaluate the dPF was the deep drawing process. Three different deep drawing processes were analyzed giving as a result different force. Compared to the stroke against two rigid steel cylinders, the deep drawing process is characterized by prolonged force profiles that begin in an earlier and end in a later angular position of the crankshaft. Furthermore the evolution of the force is not as homogeneous as it was in the case of the stroke against two rigid steel cylinders. The main purpose of these experiments was to evaluate if the prediction algorithm was able to calculate the force in real forming processes. The cadence of the servo press during these experiments was 20 strokes per minute for DD1 and DD2 and 6 strokes per minute for DD3.

Table 2 gathers the methodological set-up to carry out the three different deep drawing experiments.

IOP Conf. Series: Materials Science and Engineering **967** (2020) 012015 doi:10.1088/1757-899X/967/1/012015

Table 2. Experimental set-up of the deep drawing processes

Experiment	Maximum force measured	Adjustment of ram (height)	Angular speed during force profile	Sheet material
DD1	79.52 t	850.2 mm	120 º/s	DP1000
DD2	184.40 t	850.2 mm	120 º/s	DP1000
DD3	49.66 t	800.0 mm	36 º/s	DP1000

The estimation results of the three types of deep drawing processes are shown in Figure 5. Regarding the deviations at the maximum force position in the three experiments, the obtained deviations are 0.9254%, 2.1381% and 1.1715% for DD1, DD2 and DD3 respectively. Then, some fluctuation can be seen again in experiments DD1 and DD2, which are attributed again to the controls activity.

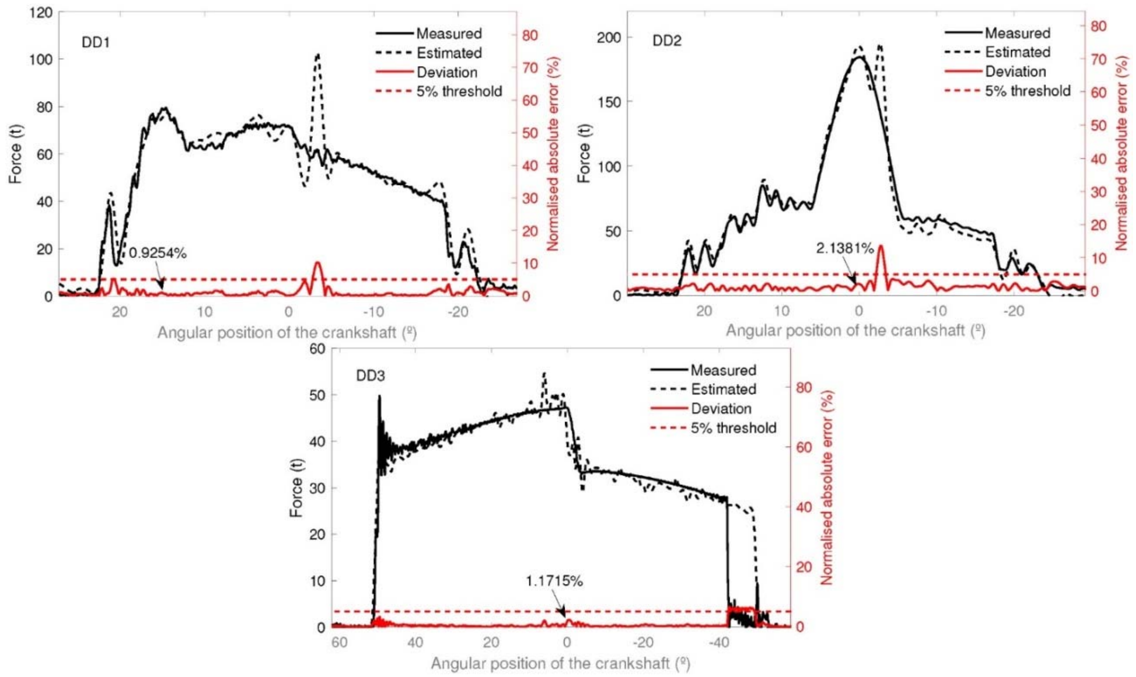

Figure 5. Measured and estimated process forces of the three deep drawing experiments and the instantaneous normalised absolute deviation.

4.3 Semi solid forging

The third process analysed at the present research work was the semi solid forging where a workpiece that is in a semisolid state is formed in a closed die. In this process the force increases until reaching the maximum value at the bottom dead centre (BDC) (lowest position of the ram), and then the ram is stopped at that position during a determined period of time forming the workpiece. The main purpose of this analysis was to evaluate the prediction capacity of the algorithm under static conditions close to the BDC of the servo press.

Table 3 gathers the methodological set-up to carry out the two different semi solid forging experiments.

Table 3. Experimental set-up of the semi solid forging processes

Experiment	Maximum force measured	Adjustment of ram (height)	Maximum force position	Angular speed during force profile	Workpiece material
SSF1	417.72 t	960.0 mm	19.12º	90 º/s	42CrMo4
SSF2	297.60 t	960.0 mm	3º	0 º/s	S48C

The results of semi solid forging experiments are shown in Figure 6. In SSF1 the maximum force of the servo press was applied before reaching the BDC, so the safety mechanism of the press switched off the servomotor around 18º angular position before reaching the BDC and therefore the estimations are not representative from that point onwards. Otherwise the normalized absolute deviation remains under the 5% threshold. Regarding the second experiment, a complete SSF operation was performed, where the ram was stopped for 6 seconds at the BDC. A significant peak is illustrated between seconds 11 and 12, which is due to control's activity to correct the speed deviation that occurs as the structure recovers from its elastic deformation.

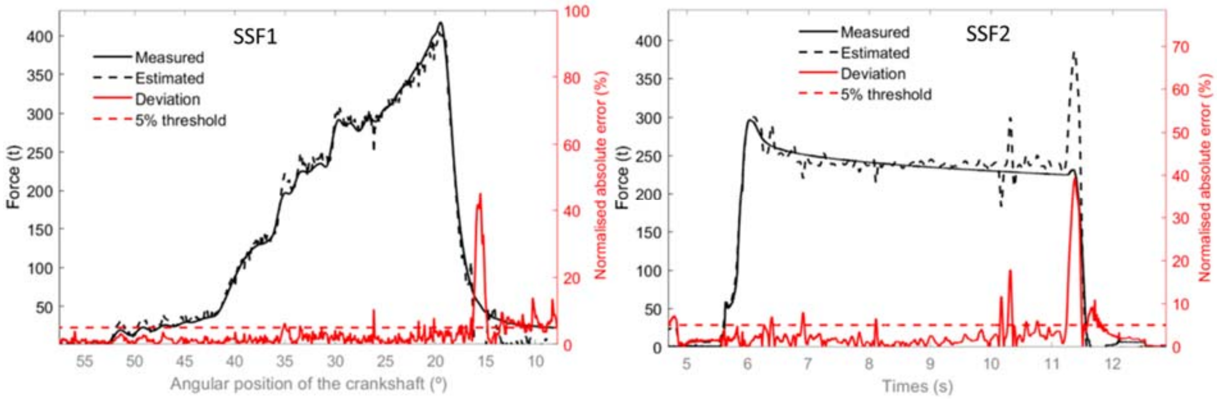

Figure 6. Measured and estimated process forces of the two semi solid forging experiments and the instantaneous normalised absolute deviation.

Based on the previous results, the proposed work could give rise to control strategies that act on the processes to improve production and the quality of the formed parts. Furthermore, the estimation of the press forces and states can also reveal information about the condition of the machine, thus allowing machine failures and downtime to be prevented. Moreover, the developed algorithm and its hardware implementation can be ported to other machines and processes by modifying the underlying model while keeping the rest of the infrastructure the same.

5. Conclusions

This paper presents experimental results of the servo press's process force obtained under three different metal forming operations applying the dPF soft sensor. The employed algorithm takes advantage of the already available signals used by the CNC, thereby avoiding the need to introduce new sensors to the system. The results show that the estimated process forces approximate well the measured force signals being the maximum error 2.97% of the measured force.

6. Acknowledgements

The technical support of Andoitz Aranburu from Fagor Arrasate S. Coop is gratefully acknowledged.

IOP Conf. Series: Materials Science and Engineering **967** (2020) 012015 doi:10.1088/1757-899X/967/1/012015

7. References

[1] T. Altan and A. E. Tekkaya, Sheet metal forming: fundamentals. Asm International, 2012

[2] R. Kumme, O. Mack, B. Bill, C. Gossweiler, H. Haab, and K. I. AG, “Dynamic properties and investigations of piezoelectric force measuring devices,” VDI Berichte, vol. 1685, pp. 161–172, 2002.

[3] R. Doraiswami and L. Cheded, “Robust model-based soft sensor: design and application,” IFAC Proceedings Volumes, vol. 47 DOI 10.3182/20140824-6-ZA-1003.00245, no. 3, pp.5491–5496, 2014

[4] J. Olaizola, C. Bouganis, E. S. de Argandoña, A. Iturrospe and J. M. Abete, "Real-Time Servo Press Force Estimation Based on Dual Particle Filter," in IEEE Transactions on Industrial Electronics, vol. 67, no. 5, pp. 4088-4097, May 2020.

[5] R. Halicioglu, L. C. Dulger, and A. T. Bozdana, “Modelling, design, and implementation of a servo press for metal-forming application,” The International Journal of Advanced Manufacturing Technology, DOI 10.1007/s00170-016-9947-8, pp. 1–12, 2016.

[6] J. Olaizola, J. M. Abete, A. Iturrospe, and E. Saenz de Argandoña, “Modelling, simulation and validation of a ram-crank servo driven press,” in 19th Scientific Convention on Engineering and Architecture, pp. 112–123, 2018.